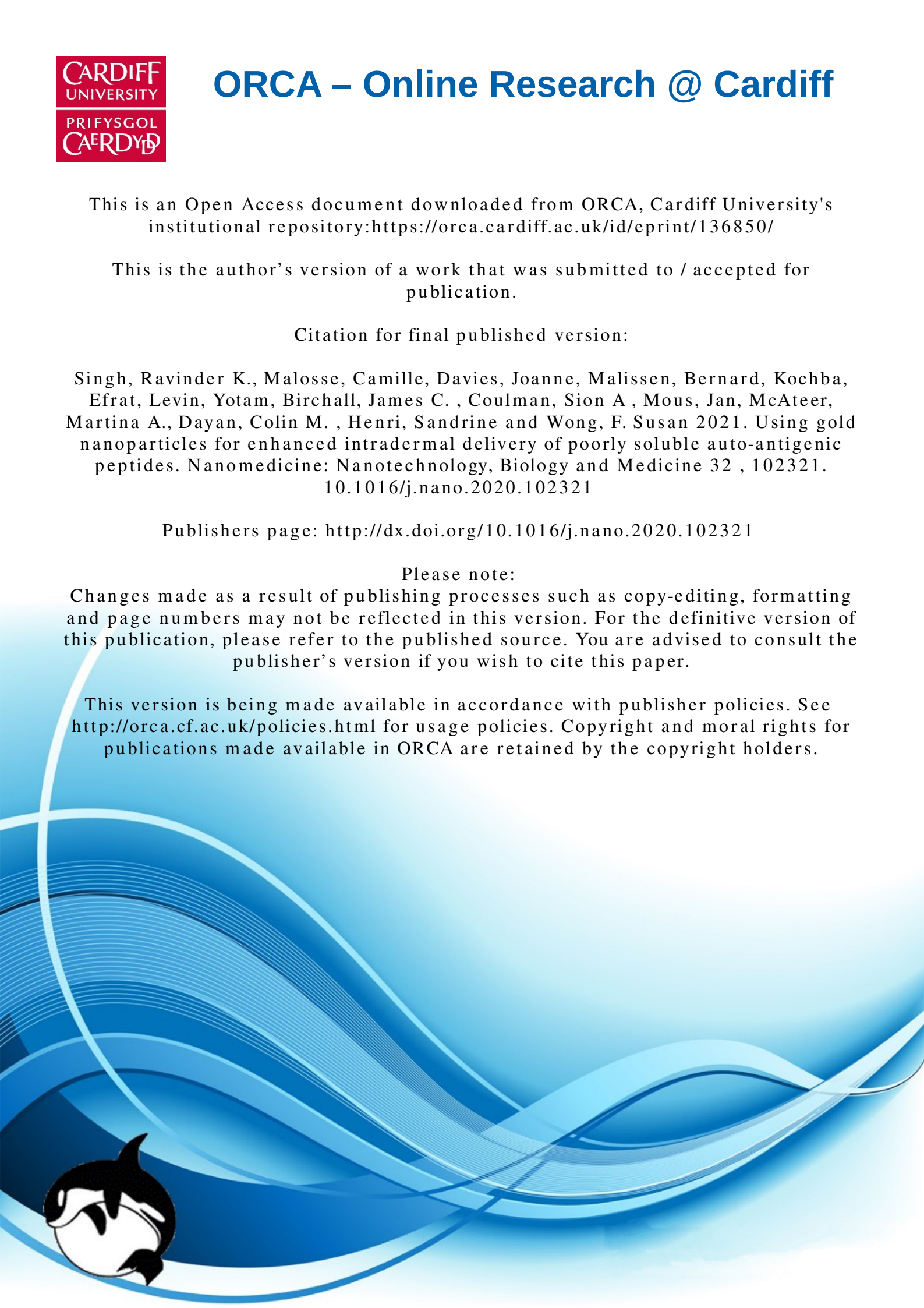

Using gold nanoparticles for enhanced intradermal delivery of poorly soluble auto-antigenic peptides

R.K Singh[a], C. Malosse[b], J. Davies[a], B. Malissen[b,c], E. Kochba[d], Y. Levin[d], J.C Birchall[e], S.A Coulman[e], J. Mous[f], M.A McAteer[f], C.M Dayan[a], S. Henri[b], F.S Wong[a]

[a] Division of Infection & Immunity, School of Medicine, Cardiff University, Heath Park, Cardiff CF14 4XN, UK

[b] Centre d'Immunologie de Marseille-Luminy, Aix Marseille Université, Inserm, CNRS, 13288 Marseille, France

[c] Centre d'Immunophénomique, Aix Marseille Université, INSERM, CNRS, 13288 Marseille, France

[d] NanoPass Technologies Ltd., Nes Ziona, Israel

[e]School of Pharmacy and Pharmaceutical Sciences, Cardiff University, UK

[f] Midatech Pharma PLC, Milton Park, Abingdon, Oxford, UK

Corresponding author: Prof. C.M.Dayan, Division of Infection & Immunity, School of Medicine, Cardiff University, Heath Park, Cardiff CF14 4XN, UK

Email dayancm@cardiff.ac.uk

Telephone: +44 2920687000

Word count: 150 words abstract, 5000 words text and legends

Number of figures: 8 Number of tables 2

Funding: This work is part of the EE-ASI European research network (Collaborative Project) supported by the European Commission under the Health Cooperation Work Programme of the 7th Framework Programme (Grant agreement n° 305305).

Conflicts of interest: none

ABSTRACT

Ultra-small 1-2nm gold nanoparticles (NP) were conjugated with a poorly-soluble peptide auto-antigen, associated with type 1 diabetes, to modify the peptide pharmacokinetics, following its intradermal delivery. Peptide distribution was characterised, in vivo, after delivery using either conventional intradermal injection or a hollow microneedle device. The poorly-soluble peptide was effectively presented in distant lymph nodes (LN), spleen and draining LN when conjugated to the nanoparticles, whereas peptide alone was only presented in the draining LN. By contrast, nanoparticle conjugation to a highly-soluble peptide did not enhance in vivo distribution. Transfer of both free peptide and peptide-NPs from the skin to LN was reduced in mice lacking lymphoid homing receptor CCR7, suggesting that both are actively transported by migrating dendritic cells to LN. Collectively, these data demonstrate that intradermally administered ultra-small gold nanoparticles can widen the distribution of poorly-soluble auto-antigenic peptides to multiple lymphoid organs, thus enhancing their use as potential therapeutics.

Key words: gold nanoparticles, hydrophobic, peptide, intradermal, microneedle, autoantigen

BACKGROUND

Type 1 diabetes is an autoimmune disease characterised by the destruction of insulin-producing beta cells within the pancreas [1]. Insulin maintains blood glucose levels but is not a cure. Hence, we seek strategies to deliver antigen-specific immunotherapy to reduce immune-mediated beta cell damage.

The skin is an accessible route for therapeutic delivery. The rich network of antigen-presenting cells, including epidermal Langerhans and dermal dendritic cells (DCs) in skin, facilitates both immune activation and regulation, upon delivery of a therapeutic [2-5]. Microneedles (MNs) are a viable alternative to conventional hypodermic needles for intradermal (ID) delivery, being both minimally invasive and relatively pain-free [6, 7]. A variety of MNs exist, including the 600µm hollow MNs (MicronJet600^{TM}), which have been used in this study and in the clinical setting to deliver insulin [8], influenza vaccine [9, 10], zoster vaccine [11] and polio [12, 13]. MicronJet600^{TM} hollow MNs reproducibly and effectively deliver material into the dermal compartment, with a significant vaccine dose sparing effect and improved immunogenicity compared with intramuscular and subcutaneous delivery [14].

Nanoparticles (NPs) can be conjugated to multiple therapeutics, including peptides, as drug delivery agents. They can protect peptides from degradation, and can form a depot at the site of injection so enhancing antigen retention and uptake by DCs. Moreover, small carbohydrate-coated gold NPs also offer reduced toxicity [15] and bio-compatibility as well as exhibiting anti-inflammatory properties [16]. Furthermore, gold (Au) can be easily and covalently decorated on its surface by exploiting the strong soft–soft interaction between Au atoms and sulfur. Therefore, gold NPs represent a versatile nanoplatform for development of epitope-based vaccines [17].

Recently, NPs have been used to prevent autoimmune diabetes in the non-obese diabetic (NOD) mouse model of diabetes by generating tolerogenic DCs and promoting T regulatory cell expansion to re-establish immune tolerance [18, 19]. Although promising, both studies utilised systemic

(intravenous or intraperitoneal) delivery systems, as well as large (>50nm) NPs. In humans, skin-mediated delivery is more practical, convenient, has fewer safety concerns and can exploit the local immune cells. We have recently demonstrated that gold NPs (Midacore™) (<5nm hydrodynamic radius), conjugated to a peptide autoantigen, can be effectively delivered into the dermal and epidermal layers of human skin explants by MicronJet600™ hollow MNs and target local antigen-presenting cells [20]. This present study is the first published report exploring the in vivo pharmacokinetics and resulting systemic immune response following MN-mediated delivery of a poorly-soluble auto-antigenic peptide conjugated to ultra-small gold NPs.

METHODS

Animal models

BDC2.5 TCR transgenic NOD mice [21] have diabetogenic CD4+ T-cells that recognise a hybrid insulin-chromogranin A peptide (HIP) [22] and mimotope peptides (the specific one used in this study is designated BDC2.5 mimotope peptide) [23]. The mice were purchased from the Jackson laboratory and have been bred in a specific pathogen-free facility of Cardiff University. OTII TCR transgenic C57BL/6J mice [24] and CCR7$^{-/-}$ mice [25] on the C57BL/6J genetic background have previously been described. C57BL/6J mice were purchased from Janvier (France). Mice were maintained in individually-ventilated filter cages in scantainers on a 12hr light/dark cycle. Animal procedures were approved by University ethical review committee. All procedures relating to NOD mice were performed in accordance with protocols approved by the UK Home Office. All procedures relating to OTII and CCR7$^{-/-}$ mice were carried out in accordance with French and European directives.

Peptides and solubility

The peptides (physiochemical properties shown in Table 1) were purchased from Peptide Synthetics, manufactured to >95% purity: BDC2.5 mimotope – YVRPLWVRME; Hybrid Insulin Peptide (HIP) – DLQTLALWSRMD; Ovalbumin323-339 peptide (OTII)-ISQAVHAAHAEINEAGR.

NP synthesis/characterisation

Gold NPs (Midacore^{TM}) with a gold core size of <5 nm were synthesised and supplied by Midatech Pharma [20]. NPs were conjugated with each of the poorly-soluble HIP and BDC2.5 peptides as well as the highly-soluble ovalbumin peptide, OTII, using custom-synthesized peptides with a thiol propionic acid linker, in an amide linkage at the N terminal (-S(CH2)2- CONH) (AmbioPharm Inc, North Augusta, SC, USA). Fig.1 illustrates the schematic structure of NPs covalently linked to BDC2.5 mimotope peptide and Table 2 summarizes the NP properties. For all reactions, gold (III) chloride was mixed with a 3-fold excess of organic ligands and peptide in different ratios (5% β glucose C2 (synthesised in-house) and either 94% or 92% L-glutathione oxidised (Sigma Aldrich) and 1% or 3% peptide). Glutathione enabled non-enzymatic intracellular activation and release. The NPs were produced by reduction, following rapid addition of a 20-fold molar excess, relative to gold, of freshly-made 1M sodium borohydride (Sigma Aldrich, Poole, UK) under vigorous vortex mixing. The samples were continuously vortexed for 1min followed by a further 1hr constant mixing on a flatbed shaker at room temperature. After 1hr, the NP samples were concentrated by ultrafiltration using Amicon Ultra-15 centrifugal filter tubes (Millipore Ltd, 10 K membrane molecular weight cut-off) and washed 4 times with Milli-Q water (4 ml) to remove unbound peptide and residual borohydride.

The NP gold content was determined using a colorimetric gold assay. Hydrodynamic size and zeta potential of the NPs in water/10% PBS was determined by dynamic light scattering (DLS) using a Zetasizer Nano ZSP (Malvern instruments). Peptide content of the NP samples was determined by HPLC using a Varian 900-LC, with a reverse phase C18 column (Acquisition time: 11.2 min;

Temperature=35°C; Slit width=2nm; 95% water, 5% acetonitrile gradient (1ml/min) switching at 8 min, switch to 20% water, 80% acetonitrile). In brief, an aliquot of NPs (10µl) was mixed with 40µl of KCN solution (100mM in 10mM potassium hydroxide) to dissolve the gold. The sample was analysed by HPLC at 212nm to determine released peptide concentration, and at 400nm to confirm that all the gold was dissolved. An aliquot of NPs (10µl), diluted with 20µl TFA, was also analysed by HPLC to determine whether any free peptide remained in the NP solution, following ultrafiltration purification.

ID injection of peptide-loaded NPs

Mice were anaesthetised using isoflurane and the injection site was shaved prior to delivery. Free peptide or peptide-loaded NPs were injected intradermally in 50µl sterile PBS using a 29G insulin needle.

MN characterisation and injection of peptide-loaded NPs

Hollow MN devices (MicronJet600^{TM}) were provided by NanoPass Technologies. MicronJet is a CE marked and FDA cleared device consisting of three MNs, each 600µm in length, with a lumen of approximately 60µm in diameter, bonded to a plastic adapter that attaches to a Luer syringe [14]. MicronJet600 ^{TM} injection did not change the diameter of NPs, which remained physically stable under the shear forces of the injection [26]. Mice were anaesthetised using isoflurane, and the injection site was shaved. Peptide was prepared and injected in 50µl sterile PBS.

Adoptive cell transfer

BDC2.5 CD4+ T-cells were separated from splenocytes using a MACS CD4 II negative selection kit (Miltenyi Biotec). Cells were labelled with 20µM CFDA (Invitrogen) in 10% foetal calf serum (FCS) RPMI at room temperature for 5min at a concentration of 10^7/ml. The cells were then washed twice

in RPMI containing FCS and rested for 15min in the same media, and subsequently washed in saline. These cells were then re-suspended at 4×10^6 cells in 200µl sterile saline and injected intravenously into 6-10-week-old female mice. At the indicated times, single-cell suspensions were prepared from spleen and various LNs, and CD4+ T-cells were analysed by FACS. OTII T-cells were isolated from pooled LNs and spleen of OTII mice maintained on a *Rag-2*$^{-/-}$xB6 [CD45.1] background using a CD4$^+$ T-cell negative isolation kit (Dynal, Invitrogen). For CTV labelling, purified OTII T-cells were resuspended in PBS containing 2.5mM cell tracer violet (CTV) (Molecular Probes) for 3min at room temperature. 10^6 CTV-labelled OTII T-cells were adoptively transferred into the specified mice.

Phenotypic analysis by flow cytometry

All antibodies were purchased from BioLegend and BD Pharmingen.

A single cell suspension was pre-treated with anti-CD16/32 (BD Pharmingen) and then stained at 4^{o}C for 25mins with the following pre-titrated mAbs against the indicated antigens: CD4-AF700 (RM4-5), CD44-BV71 (IM7), CD3e-AF700 (500A2), CD45.1-APC (A20), CD4-BV786 (RM4-5) and TCR Vα2-PE (B20.1). To assess intracellular expression, samples were permeabilised and fixed using Foxp3 transcription factor staining buffer set (eBioscience) according to the manufacturer's instructions. Intracellular mAbs against the following proteins included: CTLA4-BV421 (UC10-4B9), IL10-BV650 (JES5-16E3) and IFNγ-PeCY7 (XMG-1.2). Cell viability was evaluated using fixable viability dye efluor780 (eBioscience) or zombie yellow (Biolegend), according to the manufacturer's instructions. Samples were then washed and read using a FACS LSRII Fortessa cytometer with DIVA software (BD) and analysed using FlowJo software (Treestar).

Statistical Analysis

All results are presented as the mean±standard error of the mean (SEM) and were analysed using GraphPad Prism V5. Student's t-test, one-way ANOVA and two-way ANOVAs (for analyses with

more than 1 variable) with Bonferroni post-hoc test were used for statistical analysis. *P* values of <0.05 were considered statistically significant: *denotes p<0.05, **denotes p<0.01, ***denotes p<0.001.

RESULTS

Pharmacokinetics of intradermally-delivered BDC2.5 mimotope peptide coupled to NP differs from BDC2.5 mimotope peptide alone in vivo

Following the intravenous transfer of CFDA-labelled islet-specific BDC2.5 CD4+ T-cells into naïve NOD mice, BDC2.5 NPs, BDC2.5 peptide alone (2µg peptide in 50µl) or peptide free 'blank' NPs were administered by ID injection at the back of the neck. Lymphoid organs were then analysed at 24, 48 and 72hrs. Following administration of BDC2.5 NPs, BDC2.5 T-cell proliferation in the skin-draining LN (axillary), the non-draining LN (inguinal), the spleen and pancreatic LN (PLN) was enhanced, compared to baseline at the 48 and 72hr time points (Fig.2). In contrast, levels of proliferation were much reduced in mice treated with BDC2.5 mimotope peptide alone; proliferation was only detected in the axillary (draining) LN at the 72hr time point, with no proliferation at either 24 or 48hr (and only baseline proliferation in the PLN) (Fig.2). As expected, modest proliferation of BDC2.5 CD4+ T-cells as a result of endogenous presentation of the cognate antigen occurred in the pancreatic LN in control mice. This was not enhanced following ID injection of peptide and indicates that the peptide administered alone was not disseminated to the PLN. No proliferation was observed using peptide-free 'blank' NPs, confirming the antigen-specific nature of the response. Overall, ID delivery of BDC2.5 peptide via NPs resulted in significantly higher levels of T-cell proliferation in distant lymphoid tissues and at earlier time points than peptide alone.

Peptide NP conjugation: the effects of T-cell affinity

CD4+ T-cells are central in the process of beta cell destruction. BDC2.5 CD4+ T-cells are highly diabetogenic and the natural epitope for these pathogenic cells is a hybrid insulin peptide (HIP), formed by the fusion of a chromogranin A peptide sequence WE14 and insulin C-peptide [22]. Although naturally formed, HIP has a lower affinity for BDC2.5 CD4+ T-cells than the commonly used high affinity islet antigenic peptide substitute BDC2.5 mimotope. Therefore, to determine whether NP conjugation changed these relative peptide affinities, NPs were conjugated to either the high affinity BDC2.5 mimotope peptide or the lower affinity naturally-formed HIP peptide. CFDA-labelled BDC2.5 CD4+ T-cells were then intravenously transferred into NOD mice and these mice were subsequently treated with an ID injection of an NP formulation (BDC2.5 mimotope or HIP peptide or peptide alone. At 72hours, proliferation of transferred BDC2.5 CD4 T-cells was significantly higher in all lymphoid tissues following treatment with the BDC2.5 NPs compared to BDC2.5 peptide (Fig.3A and B), replicating earlier findings shown in Fig.2. However, this effect was not observed using the lower affinity HIP-NPs at an equivalent peptide dose (2µg). Instead, HIP-NPs only induced proliferation in the axillary LN and at lower levels than those seen with BDC2.5-NP, though still significantly higher than HIP peptide alone. Endogenous proliferation in the pancreatic LN was not enhanced by 2µg HIP-NP. No proliferation above control (no ID injection) was observed in the inguinal LN and spleen. However, when a higher dose of HIP-NP was administered (10µg), widespread proliferation was observed in these NP-treated mice, with profiles resembling those witnessed with 2µg BDC2.5 NP. These results are consistent with lower amounts of peptide-NP being present in distant LN and in the case of a lower affinity peptide, may be limiting for T-cell proliferation at lower doses. Dissemination of peptide alone was much less efficient than its NP-formulated counterpart and therefore no presentation was witnessed in the distant LNs, at any of the doses of HIP peptide that were examined.

Peptide-NP conjugation: effects of peptide solubility

The influence of peptide solubility on peptide-NP behaviour was also evaluated in vivo (Fig.4), by comparing the behaviour of the highly water-soluble OTII peptide, recognised by OTII CD4+ T-cells, with the less soluble BDC2.5 and HIP peptide counterparts. CTV-labelled cells were transferred into C57BL/6 mice, followed by OTII peptide or OTII-NP at 2µg or 10µg by ID injection, using 29G insulin needles. At a 2µg OTII-NP dose, T-cell proliferation occurred in all the lymphoid organs, with greatest proliferation in the draining lymph nodes (brachial and axillary LN). Moreover, at the higher dose of 10µg, OTII-NP induced significantly more T-cell proliferation than 2µg OTII-NP in the inguinal LN (**$p<0.01$) and spleen (***$p<0.001$). In contrast to both BDC2.5 and HIP peptide, proliferation of T-cells in response to the OTII peptide also reached almost 100%.

Peptide-NP can be successfully delivered via MicronJet600^{TM} microneedles into murine skin

To test whether using MicronJet600^{TM} MNs would enhance peptide-NP and free peptide delivery in vivo, experiments were performed in both NOD and C57BL/6 mice. Following intravenous transfer of BDC2.5 CD4+ T-cells into NOD mice (Fig.5), and OTII cells into C57BL/6 mice (Fig.6), the respective mice were injected with 2µg BDC2.5-NP or 2µg OTII peptide-NP or soluble peptide using MicronJet MNs. Lymphoid organs were harvested after 72hrs and proliferation was analysed. Figs.5 and 6 indicate successful peptide-NPs delivery using MNs, with high levels of proliferation in the skin-draining brachial and axillary LN, as well as the inguinal LN and spleen, thus confirming and presentation of the MN-delivered antigen to the responding T-cells. However, the use of MicronJet needles, in this context, did not enhance delivery of the BDC2.5 peptide alone, nor alter the delivery of OTII peptide compared to conventional ID injection. Overall, proliferation following MN delivery was comparable to that observed with conventional ID injection.

Peptide-NP is transported to LN by migratory skin DCs

CCR7, a leukocyte chemotactic receptor, is expressed by mature DCs and plays a key role in DC homing to LNs, as well as their subsequent positioning within LN functional compartments. Loss of

CCR7 impedes DC migration from non-lymphoid organs, such as the skin, into the draining LN [25, 27]. With this in mind, CCR7-deficient mice were used to determine the role of DCs in distribution of OTII peptide and OTII peptide-NP, and to determine whether peptide transport is an active DC-mediated process. ID injection of OTII peptide and OTII-NP were therefore examined at two different concentrations (2µg and 10µg) in wild type C57BL/6 or CCR7KO C57BL/6 mice. A reduction in proliferation was observed in different LN of the CCR7KO mice following administration of the peptide-NP, with a significant reduction at the higher 10µg OTII concentration in both the draining LN and spleen (*$p<0.05$) (Fig.7). Although the same trend was observed with 2µg OTII-NP and peptide alone, the decrease was not statistically significant. This suggests that migratory DCs are important for peptide-NP transport from the skin to the draining LNs, particularly at high concentrations.

HIP-NP influences cellular phenotype in a concentration-dependent manner

To determine the impact of HIP-NP concentration on cell function, NOD mice were transferred with CFDA-labelled BDC2.5 CD4+ T-cells and then immediately treated with an ID injection of 0.4µg, 2µg, 6µg or 10µg HIP-NP or free HIP peptide. After 72hrs, axillary draining LNs, the inguinal LN, spleen and pancreatic LN were harvested, examined and a concentration dependent HIP-NP proliferative response was revealed. Proliferation in the axillary LN, inguinal LN and spleen, were most notable at 10µg. This was significantly higher than the proliferation observed in the HIP peptide- administered mice (Fig.8a) and consistent with experiments that were conducted with a more limited dose range (Fig.3). Furthermore, the axillary LN T-cells expressed increased levels of activation markers CD44 and CTLA4 (Fig.8b), which reached significance at lower concentrations compared with proliferation in the inguinal LN and spleen. Despite enhanced activation status, a significant decrease in cells expressing IFNγ was noted in the axillary LN of HIP-NP treated mice compared to peptide alone (*$p<0.05$). IL-10 expression was low under all conditions (Fig.8c).

Therefore, whilst T-cells displayed an increased activation and proliferation profile over a wide HIP-NP range, functionally the cells of the draining LN produced less IFNγ.

Discussion

The lipophilicity of 'naked' peptide autoantigens has been shown to influence localised delivery in human skin [28]; results in murine skin (Figs.2-6) provide further exemplification of this. The murine dermis is an aqueous region, consisting of 60.3% water [29], and therefore the notable increase in T-cell proliferation in response to intradermal administration of the water-soluble OTII peptide (its cognate antigen) at lymphoid organs distant to the local environment (Fig.7) is likely to be facilitated by rapid diffusion in the local environment, uptake by DC in draining LNs and subsequent distribution in the lymphatic system. However more lipophilic auto-antigenic peptides such as BDC2.5 and HIP, which are insoluble in aqueous media, such as water and PBS, are only able to stimulate response in the local environment i.e. in the draining lymph node (Figs.2-3). Enhancing the distribution of poorly water-soluble peptides to stimulate immune responses distant from their administration site may be desirable for a range of therapeutic approaches, including immunotherapy for conditions such as Type 1 diabetes.

Gold NPs have recently garnered attention as drug delivery agents for several reasons, including their lack of toxicity [31], chemical stability and extensive surface to volume ratio [32, 33], which enables conjugation of clinically significant doses of therapeutics. NPs have previously been used to deliver disease-relevant autoantigens in mouse models of EAE [34-36], arthritis [37, 38] and diabetes [18, 19, 39]. Therefore, in this study we have explored the potential of a gold NP formulation to enhance trafficking of lipophilic peptides from the antigen-presenting cell (APC) rich skin compartment to distant target sites, such as the pancreas and pancreatic LN. We have also investigated the

importance of the mechanism of administration (microneedles versus ID injection), peptide affinity, peptide solubility and dosing on peptide-NP trafficking in vivo.

Peptide-NPs incorporating the relatively insoluble BDC2.5 and HIP peptides facilitated enhanced proliferation at LNs distant to the site of intradermal injection, thus indicating a marked improvement in distribution, in vivo, compared to peptide alone. Enhanced proliferation of T-cells, in response to the NP-conjugated lipophilic peptides, was detectable in the draining LN, the non-draining LN, the spleen and the PLN, 48hours after intradermal administration. These kinetics are consistent with a minimum requirement of 24hrs for T-cell proliferation to occur after antigen encounter. Conversely, conjugation of the highly water-soluble OTII peptide to the NP formulation reduced proliferation in the LNs at a "like for like" dose (2μg) and it was only at an increased dose (10μg) that the NP formulation performed comparably to the 'naked' peptide. This may be explained by a reduction in the diffusive properties of the hydrophilic peptide upon conjugation to a gold NP and, as a corollary, indicates that the enhancement afforded by conjugation of the lipophilic peptides to the ultra small gold NPs may not be mediated simply by an increase in the solubility and diffusive properties of the therapeutic within the tissue. However, whilst these results are indicative, the lipophilic and hydrophilic peptides used in this study are detected by two different T-cell clones in two different mouse strains. Future experiments examining a range of peptide solubilities in a single mouse strain are therefore needed to probe this hypothesis further. Further studies could also explore whether NP-conjugation affords any enhancements in peptide stability in vivo, as this may also contribute to enhanced and prolonged T-cell proliferation.

DCs are abundant in the immunocompetent skin. Increased peptide uptake by DCs in the local environment is more likely to result in increased activation and translocation of these highly effective APCs from the skin to the draining LNs and subsequent presentation to their cognate T-cells. Studies conducted in the CCR7-deficient mouse model at high OTII-NP concentrations (Fig.7) were

therefore used to probe the role of DCs in trafficking locally-delivered NP-conjugated lipophilic peptides to distant LNs. Data indicate that distribution to LNs was partly dependent on DCs, with those mice lacking the lymph node homing receptor, CCR7, displaying reduced proliferation in response to peptide-NP administration (Fig.7). Previous studies suggest that intradermally-delivered antigens conjugated to a NP formulation diffuse within the extracellular environment to the draining LN for presentation to resident DCs in a size-dependent manner [5, 42, 43, 45, 46]. Furthermore, it has been hypothesised that 'large' NPs, ranging from 33nm [45] to 500nm [46], are internalised by DCs at the site of injection and are trafficked to local LNs for presentation, whilst 'small' NPs are not retained in LNs, thereby reducing the magnitude and quality of the ensuing T-cell response [45, 47] and Foxp3 T-reg induction [43, 48]. In contrast to this, we have shown that ultra-small OTII-NPs (2-6nm) are, in part, taken up by DCs following ID injection and are subsequently transported to the local draining LN. Mice deficient in the LN homing receptor CCR7 demonstrated significantly less proliferation in the draining LN, particularly at the high concentration peptide-NP formulation. We therefore hypothesise that the enhancement in the distribution afforded by gold NP conjugation to poorly soluble peptides is, in part, due to enhanced trafficking from the site of injection by DCs, rather than simply by a change to the diffusive properties of the formulation. This finding is of particular interest, as it implies that peptide-NPs could be formulated with a second tolerogenic cargo that could be targeted and co-delivered to skin DCs (rather than those LN resident DCs that may be responsible for presentation of 'naked' peptide that reaches the LN by diffusion), thus potentially enabling DC function to be modulated prior to migration to the draining LN.

Different affinities of the peptides to their corresponding antigen-specific T-cells resulted in observable differences in the in vivo response to the BDC2.5, HIP and OTII peptide-bound NP formulations. BDC2.5 mimotope peptide, identified by screening a peptide library [23], has a high affinity to BDC2.5 CD4+ T-cells whereas HIP, a relatively newly-discovered peptide epitope, has been proposed as the natural peptide for the highly diabetogenic BDC2.5 T-cells and thus, in

common with many autoantigens, is relatively lower affinity [22]. This relationship was maintained following NP conjugation of the peptides, with HIP-NPs inducing less proliferation than BDC2.5-NPs at the same peptide dose, thus indicating that NP conjugation to the peptide does not have a detrimental effect on the relative potencies of these auto-antigens.

Previous studies using NPs formulated with an islet autoantigen provide evidence that enhanced expansion of regulatory T-cells in lymphoid organs may translate to a tolerogenic response in diabetes mouse models [18, 19]. This was exemplified by an expansion in T regulatory cells and suppression of diabetes development; however neither study delivered antigen by the intradermal route [18, 19]. In both of these studies the authors reasoned that NPs would also benefit from a second tolerance-inducing cargo. Indeed, sub-cutaneous delivery of antigen-specific NP formulations, intended to induce tolerance in vivo, have typically used additional anti-inflammatory mediators, such as IL10 [42], rapamycin [34] or TGFβ [43]. HIP-NP studies were therefore extended to explore whether intradermal delivery and enhanced distribution of the peptide to distant LNs could bring about a phenotypic change that is indicative of tolerance in Type 1 diabetes i.e. a reduction in IFNγ, a pro-inflammatory cytokine whose levels correlate with disease progression and which is known to enhance the development of type 1 diabetes in the NOD mouse model [40, 41]. Down-regulation of this pro-inflammatory mediator IFNγ, three days after administration of HIP-NPs (Fig.7), therefore encourages further investigation of HIP-NP as a therapeutic candidate, potentially a pro-tolerogenic addition to the NP formulation to further enhance regulation.

In this study, NPs were administered via an ID injection using both traditional hypodermic needles and hollow MNs (MicronJet600$^{TM)}$. In the mouse model, both methods were able to deliver both peptide and peptide NP formulations into the skin and facilitated comparable in vivo responses. Whilst there are well-recognised differences in murine and human skin, here, both methods of delivery proved equal in their ability to deliver peptide and peptide-NP. Both methods are easily

translatable to humans, and peptide and peptide-NP are presented in LNs distant to the site of injection [9].

In conclusion, this study illustrates the potential value of the intradermal delivery of ultra-small gold NPs for enhanced delivery of lipophilic peptide autoantigens to lymphoid organs and the importance of peptide dose, affinity and solubility on distribution to, and T-cell expansion at, these body sites. Peptide-NP formulations therefore potentially provide a valuable means of targeting poorly soluble peptide epitopes to internal directly inaccessible LNs, such as the pancreatic LN, which may be of particular value in Type 1 diabetes tolerisation strategies. Future studies will investigate the clinical utility of this drug delivery system in immunotherapy.

References

[1] M.S. Anderson, J.A. Bluestone, The NOD mouse: a model of immune dysregulation, Annu Rev Immunol, 23 (2005) 447-485.

[2] M. Guilliams, S. Henri, S. Tamoutounour, L. Ardouin, I. Schwartz-Cornil, M. Dalod, B. Malissen, From skin dendritic cells to a simplified classification of human and mouse dendritic cell subsets, Eur J Immunol, 40 (2010) 2089-2094.

[3] S. Henri, M. Guilliams, L.F. Poulin, S. Tamoutounour, L. Ardouin, M. Dalod, B. Malissen, Disentangling the complexity of the skin dendritic cell network, Immunol Cell Biol, 88 (2010) 366-375.

[4] N. Romani, V. Flacher, C.H. Tripp, F. Sparber, S. Ebner, P. Stoitzner, Targeting Skin Dendritic Cells to Improve Intradermal Vaccination, Current topics in microbiology and immunology, 351 (2012) 113-138.

[5] N. Romani, M. Thurnher, J. Idoyaga, R.M. Steinman, V. Flacher, Targeting of antigens to skin dendritic cells: possibilities to enhance vaccine efficacy, Immunol Cell Biol, 88 (2010) 424-430.

[6] J. Gupta, S.S. Park, B. Bondy, E.I. Felner, M.R. Prausnitz, Infusion pressure and pain during microneedle injection into skin of human subjects.

[7] S. Coulman, C. Allender, J. Birchall, Microneedles and other physical methods for overcoming the stratum corneum barrier for cutaneous gene therapy, Crit Rev Ther Drug Carrier Syst, 23 (2006) 205-258.

[8] E. Kochba, Y. Levin, I. Raz, A. Cahn, Improved Insulin Pharmacokinetics Using a Novel Microneedle Device for Intradermal Delivery in Patients with Type 2 Diabetes, Diabetes Technol Ther, 18 (2016) 525-531.

[9] Y. Levin, E. Kochba, R. Kenney, Clinical evaluation of a novel microneedle device for intradermal delivery of an influenza vaccine: are all delivery methods the same?, Vaccine, 32 (2014) 4249-4252.

[10] Y. Levin, E. Kochba, G. Shukarev, S. Rusch, G. Herrera-Taracena, P. van Damme, A phase 1, open-label, randomized study to compare the immunogenicity and safety of different administration routes and doses of virosomal influenza vaccine in elderly, Vaccine, 34 (2016) 5262-5272.

[11] C.R. Beals, R.A. Railkar, A.K. Schaeffer, Y. Levin, E. Kochba, B.K. Meyer, R.K. Evans, E.A. Sheldon, K. Lasseter, N. Lang, A. Weinberg, J. Canniff, M.J. Levin, Immune response and reactogenicity of intradermal administration versus subcutaneous administration of varicella-zoster virus vaccine: an exploratory, randomised, partly blinded trial, Lancet Infect Dis, 16 (2016) 915-922.

[12] S.B. Troy, D. Kouiavskaia, J. Siik, E. Kochba, H. Beydoun, O. Mirochnitchenko, Y. Levin, N. Khardori, K. Chumakov, Y. Maldonado, Comparison of the Immunogenicity of Various Booster Doses of Inactivated Polio Vaccine Delivered Intradermally Versus Intramuscularly to HIV-Infected Adults, J Infect Dis, 211 (2015) 1969-1976.

[13] A. Anand, K. Zaman, C.F. Estivariz, M. Yunus, H.E. Gary, W.C. Weldon, T.I. Bari, M. Steven Oberste, S.G. Wassilak, S.P. Luby, J.D. Heffelfinger, M.A. Pallansch, Early priming with inactivated

poliovirus vaccine (IPV) and intradermal fractional dose IPV administered by a microneedle device: A randomized controlled trial, Vaccine, 33 (2015) 6816-6822.

[14] Y. Levin, E. Kochba, I. Hung, R. Kenney, Intradermal vaccination using the novel microneedle device MicronJet600: Past, present, and future, Hum Vaccin Immunother, 11 (2015) 991-997.

[15] B. Fadeel, A.E. Garcia-Bennett, Better safe than sorry: Understanding the toxicological properties of inorganic nanoparticles manufactured for biomedical applications, Adv Drug Deliv Rev, 62 (2010) 362-374.

[16] R.F.J. de Araujo, A.A. de Araujo, J.B. Pessoa, F.P. Freire Neto, G.R. da Silva, A.L. Leitao Oliveira, T.G. de Carvalho, H.F. Silva, M. Eugenio, C. Sant'Anna, L.H. Gasparotto, Anti-inflammatory, analgesic and anti-tumor properties of gold nanoparticles, Pharmacol Rep, 69 (2017) 119-129.

[17] F. Compostella, O. Pitirollo, A. Silvestri, L. Polito, Glyco-gold nanoparticles: synthesis and applications, Beilstein J Org Chem, 13 (2017) 1008-1021.

[18] A. Yeste, M.C. Takenaka, I.D. Mascanfroni, M. Nadeau, J.E. Kenison, B. Patel, A.M. Tukpah, J.A. Babon, M. DeNicola, S.C. Kent, D. Pozo, F.J. Quintana, Tolerogenic nanoparticles inhibit T-cell-mediated autoimmunity through SOCS2, Sci Signal, 9 (2016) ra61.

[19] X. Clemente-Casares, J. Blanco, P. Ambalavanan, J. Yamanouchi, S. Singha, C. Fandos, S. Tsai, J. Wang, N. Garabatos, C. Izquierdo, S. Agrawal, M.B. Keough, V.W. Yong, E. James, A. Moore, Y. Yang, T. Stratmann, P. Serra, P. Santamaria, Expanding antigen-specific regulatory networks to treat autoimmunity, Nature, 530 (2016) 434-440.

[20] M. Dul, T. Nikolic, M. Stefanidou, M.A. McAteer, P. Williams, J. Mous, B.O. Roep, E. Kochba, Y. Levin, M. Peakman, F.S. Wong, C.M. Dayan, D. Tatovic, S.A. Coulman, J.C. Birchall, Conjugation of a peptide autoantigen to gold nanoparticles for intradermally administered antigen specific immunotherapy, Int J Pharm, 562 (2019) 303-312.

[21] J.D. Katz, B. Wang, K. Haskins, C. Benoist, D. Mathis, Following a diabetogenic T-cell from genesis through pathogenesis, Cell, 74 (1993) 1089-1100.

[22] T. Delong, T.A. Wiles, R.L. Baker, B. Bradley, G. Barbour, R. Reisdorph, M. Armstrong, R.L. Powell, N. Reisdorph, N. Kumar, C.M. Elso, M. DeNicola, R. Bottino, A.C. Powers, D.M. Harlan, S.C. Kent, S.I. Mannering, K. Haskins, Pathogenic CD4 T-cells in type 1 diabetes recognize epitopes formed by peptide fusion, Science, 351 (2016) 711-714.

[23] V. Judkowski, C. Pinilla, K. Schroder, L. Tucker, N. Sarvetnick, D.B. Wilson, Identification of MHC class II-restricted peptide ligands, including a glutamic acid decarboxylase 65 sequence, that stimulate diabetogenic T-cells from transgenic BDC2.5 nonobese diabetic mice, J Immunol, 166 (2001) 908-917.

[24] M.J. Barnden, J. Allison, W.R. Heath, F.R. Carbone, Defective TCR expression in transgenic mice constructed using cDNA-based [agr]- and [bgr]-chain genes under the control of heterologous regulatory elements, Immunol Cell Biol, 76 (1998) 34-40.

[25] R. Forster, A. Schubel, D. Breitfeld, E. Kremmer, I. Renner-Muller, E. Wolf, M. Lipp, CCR7 coordinates the primary immune response by establishing functional microenvironments in secondary lymphoid organs, Cell, 99 (1999) 23-33.

[26] M. Dul, M. Stefanidou, P. Porta, J. Serve, C. O'Mahony, B. Malissen, S. Henri, Y. Levin, E. Kochba, F.S. Wong, C. Dayan, S.A. Coulman, J.C. Birchall, Hydrodynamic gene delivery in human skin using a hollow microneedle device, J Control Release, 265 (2017) 120-131.

[27] R. Förster, A.C. Davalos-Misslitz, A. Rot, CCR7 and its ligands: balancing immunity and tolerance.

[28] X. Zhao, S.A. Coulman, S.J. Hanna, F.S. Wong, C.M. Dayan, J.C. Birchall, Formulation of hydrophobic peptides for skin delivery via coated microneedles, J Control Release, 265 (2017) 2-13.

[29] V. Suntzeff, C. Carruthers, The water content in the epidermis of mice undergoing carcinogenesis by methylcholanthrene, Cancer Res, 6 (1946) 574-577.

[30] R.M. Steinman, D. Hawiger, M.C. Nussenzweig, Tolerogenic dendritic cells, Annu Rev Immunol, 21 (2003) 685-711.

[31] B. Merchant, Gold, the noble metal and the paradoxes of its toxicology, Biologicals, 26 (1998) 49-59.

[32] M.U. Farooq, V. Novosad, E.A. Rozhkova, H. Wali, A. Ali, A.A. Fateh, P.B. Neogi, A. Neogi, Z. Wang, Gold Nanoparticles-enabled Efficient Dual Delivery of Anticancer Therapeutics to HeLa Cells, Sci Rep, 8 (2018) 2907.

[33] E.C. Dreaden, L.A. Austin, M.A. Mackey, M.A. El-Sayed. Size matters: gold nanoparticles in targeted cancer drug delivery. Ther Deliv. 3(4) (2012) 457-478.

[34] R.A. Maldonado, R.A. LaMothe, J.D. Ferrari, A.H. Zhang, R.J. Rossi, P.N. Kolte, A.P. Griset, C. O'Neil, D.H. Altreuter, E. Browning, L. Johnston, O.C. Farokhzad, R. Langer, D.W. Scott, U.H. von Andrian, T.K. Kishimoto, Polymeric synthetic nanoparticles for the induction of antigen-specific immunological tolerance, Proc Natl Acad Sci U S A, 112 (2015) E156-165.

[35] A. Yeste, M. Nadeau, E.J. Burns, H.L. Weiner, F.J. Quintana, Nanoparticle-mediated codelivery of myelin antigen and a tolerogenic small molecule suppresses experimental autoimmune encephalomyelitis, Proc Natl Acad Sci U S A, 109 (2012) 11270-11275.

[36] R. Kuo, E. Saito, S.D. Miller, L.D. Shea, Peptide-Conjugated Nanoparticles Reduce Positive Co-stimulatory Expression and T cell Activity to Induce Tolerance, Mol Ther, 25 (2017) 1676-1685.

[37] W.U. Kim, W.K. Lee, J.W. Ryoo, S.H. Kim, J. Kim, J. Youn, S.Y. Min, E.Y. Bae, S.Y. Hwang, S.H. Park, C.S. Cho, J.S. Park, H.Y. Kim, Suppression of collagen-induced arthritis by single administration of poly(lactic-co-glycolic acid) nanoparticles entrapping type II collagen: a novel treatment strategy for induction of oral tolerance, Arthritis Rheum, 46 (2002) 1109-1120.

[38] H.J. Kim, S.M. Lee, K.H. Park, C.H. Mun, Y.B. Park, K.H. Yoo, Drug-loaded gold/iron/gold plasmonic nanoparticles for magnetic targeted chemo-photothermal treatment of rheumatoid arthritis, Biomaterials, 61 (2015) 95-102.

[39] S. Prasad, T. Neef, D. Xu, J.R. Podojil, D.R. Getts, L.D. Shea, S.D. Miller, Tolerogenic Ag-PLG nanoparticles induce tregs to suppress activated diabetogenic CD4 and CD8 T-cells, J Autoimmun, 89 (2017) 112-124.

[40] N.C. Schloot, P. Hanifi-Moghaddam, C. Goebel, S.V. Shatavi, S. Flohe, H. Kolb, H. Rothe, Serum IFN-gamma and IL-10 levels are associated with disease progression in non-obese diabetic mice, Diabetes Metab Res Rev, 18 (2002) 64-70.

[41] M.G. von Herrath, M.B. Oldstone, Interferon-gamma is essential for destruction of beta cells and development of insulin-dependent diabetes mellitus, J Exp Med, 185 (1997) 531-539.

[42] S.T. Reddy, A. Rehor, H.G. Schmoekel, J.A. Hubbell, M.A. Swartz, In vivo targeting of dendritic cells in lymph nodes with poly(propylene sulfide) nanoparticles, J Control Release, 112 (2006) 26-34.

[43] R.M. Pearson, L.M. Casey, K.R. Hughes, L.Z. Wang, M.G. North, D.R. Getts, S.D. Miller, L.D. Shea, Controlled Delivery of Single or Multiple Antigens in Tolerogenic Nanoparticles Using Peptide-Polymer Bioconjugates, Mol Ther, 25 (2017) 1655-1664.

[44] B. Pamornpathomkul, A. Wongkajornsilp, W. Laiwattanapaisal, T. Rojanarata, P. Opanasopit, T. Ngawhirunpat, A combined approach of hollow microneedles and nanocarriers for skin immunization with plasmid DNA encoding ovalbumin, International Journal of Nanomedicine, 12 (2017) 885-898.

[45] S. Kang, S. Ahn, J. Lee, J.Y. Kim, M. Choi, V. Gujrati, H. Kim, J. Kim, E.C. Shin, S. Jon, Effects of gold nanoparticle-based vaccine size on lymph node delivery and cytotoxic T-lymphocyte responses, J Control Release, 256 (2017) 56-67.

[46] V. Manolova, A. Flace, M. Bauer, K. Schwarz, P. Saudan, M.F. Bachmann, Nanoparticles target distinct dendritic cell populations according to their size, Eur J Immunol, 38 (2008) 1404-1413.
[47] I.C. Kourtis, S. Hirosue, A. de Titta, S. Kontos, T. Stegmann, J.A. Hubbell, M.A. Swartz, Peripherally administered nanoparticles target monocytic myeloid cells, secondary lymphoid organs and tumors in mice, PLoS One, 8 (2013) e61646.
[48] R.M. Pearson, L.M. Casey, K.R. Hughes, S.D. Miller, L.D. Shea, In vivo reprogramming of immune cells: Technologies for induction of antigen-specific tolerance, Adv Drug Deliv Rev, 114 (2017) 240-255.

Figure legends

Figure 1- Gold NP composition. Composition of gold NPs used, comprising a gold core, conjugated via sulphur bonds to an organic layer of glucose or mannose, glutathione and peptide, (BDC2.5 mimotope).

Figure 2- In vivo proliferation time course analysis following peptide-NP delivery compared to peptide alone. CFDA-labelled BDC2.5 CD4+ T-cells were transferred intravenously into NOD mice, followed by an ID injection of either 2µg BDC2.5 mimotope or BDC2.5-NP or peptide free 'blank' NP. Experimental control mice did not receive the ID injection. LNs (axillary, inguinal and pancreatic) and spleen were harvested at 24, 48 and 72hours following injection and BDC2.5 CD4+ T-cells analysed for proliferation by CFSE dilution. Mean±SEM with 3 mice per treatment are shown, representative of 3 experiments. Statistical analysis was done by two-way ANOVA with Bonferroni post-test comparing BDC2.5 NP to BDC2.5 peptide (***$p<0.001$).

Figure 3- Peptide-NP effects on in vivo T-cell proliferation are dependent on peptide affinity. CFDA-labelled BDC2.5 CD4+ T-cells were transferred intravenously into NOD mice, followed by

an ID injection of peptide or peptide-NP. LNs (axillary, inguinal and pancreatic) and spleen were harvested 72hours later and proliferation analyzed by flow cytometry. (A) Representative flow cytometric plots showing proliferative responses from left to right, 2µg BDC2.5-NP, 2µg BDC2.5 peptide, 2µg HIP-NP, 2µg HIP peptide, 10µg HIP-NP, 10µg HIP peptide and no ID injection. (B) Left to right, summary of proliferation for high affinity BDC2.5 mimotope and lower affinity 2µg and 10µg HIP epitope. Mean±SEM of 3 mice per treatment are shown, representative of 3 experiments. Statistical analysis was done using one-way ANOVA with Bonferroni post-test comparing peptide-NP to peptide and control (**p<0.01, ***p<0.001).

Figure 4- Peptide-NP effects in vivo differ according to peptide solubility. (A) Representative flow cytometric plots showing proliferative responses to (from left to right) 2µg OTII-NP, 10µg OTII-NP, 2µg OTII peptide and controls in the brachial and axillary LNs (draining), distal inguinal lymph node and spleen. (B) Summary of proliferation for OTII-NP and peptide by % proliferation and absolute numbers. Data represent mean±SEM (% proliferation) and each dot corresponds to a mouse (Absolute Numbers per organ). Data are representative of three experiments with n=2-3 animals per group. Statistical analysis was done using one-way ANOVA with Bonferroni post-test comparing peptide-NP to peptide (*p<0.05 **p<0.01, ***p<0.001).

Figure 5- MicronJet600™ delivery of BDC2.5 peptide-NP and peptide alone induce proliferation of transferred T-cells. Mice received fluorescently-labelled cells intravenously, followed by an ID injection of peptide or peptide-NP using the short (600µm) hollow MN device (MicronJet600TM). Lymph nodes were harvested 72hours later and proliferation analysed by flow cytometry. (A) Representative flow cytometric plots showing proliferative responses to 2µg BDC2.5 NP vs 2µg BDC2.5 mimotope vs no MN injection. (B) Summary of cellular proliferation following administration of BDC2.5-NP or BDC2.5 peptide by MN. Mean±SEM are shown, representative of 2 experiments (n= 3 mice per treatment). Statistical analysis was done using one-way ANOVA with Bonferroni post-test comparing peptide-NP to peptide and control (**p<0.01 ***p<0.001).

Figure 6- MicronJet600™ delivery of OTII peptide-NP and peptide alone induce proliferation of transferred T-cells. Mice received fluorescently-labelled cells intravenously, followed by an ID injection of peptide or peptide-NP using the short (600µm) hollow MN device (MicronJet600TM). Lymph nodes were harvested 72hours later and proliferation analysed by flow cytometry. (A) Representative flow cytometric plots showing proliferative responses to 2µg OTII-NP, 2µg OTII peptide and controls in the brachial and axillary lymph nodes (draining), distal inguinal lymph node and spleen following MN delivery. (B) Summary of proliferation for OTII-NP and peptide. Mean±SEM (% proliferation) are shown and each dot corresponds to a mouse (Absolute Numbers per organ). Data are representative of three experiments with n=2-3 animals per group. Significant differences were identified using one-way ANOVA with Bonferroni post-test comparing peptide-NP to peptide and control (**p<0.01 ***p<0.001).

Figure 7- Peptide-NP is taken up by dendritic cells and distributed to lymphoid organs. WT and CCR7KO mice received CTV-labelled OTII T-cells intravenously, followed by an ID injection of peptide or peptide-NP using a 600µm MicronJet600™ needle. LNs and spleen were harvested 72hours later and proliferation analysed by flow cytometry. (A) Representative flow cytometric plots showing proliferative responses (left to right) to 2µg OTII-NP, 10µg OTII-NP, 2µg OTII peptide and controls in the brachial and axillary LN (draining), distal inguinal LN and spleen. (B) Absolute numbers of proliferating OTII CD4+ T-cells in response to OTII-NP and peptide. Each dot corresponds to a mouse and the mean (horizontal bar) is indicated. Data are representative of three experiments with n=2-3 animals per group. Statistical analysis was done using Student's t test comparing peptide-NP to peptide (*p<0.05).

Figure 8- HIP-NP has differential effects on the cellular phenotype dependent on concentration. NOD mice received CFDA-labelled BDC2.5 CD4+ T-cells intravenously, followed immediately by an ID injection (29G insulin needle) of HIP-NP or HIP peptide at various concentrations. LNs were harvested 72hours later and CD4+ T-cells analysed by flow cytometry.

(A) Proliferative response of cells to HIP-NP or peptide as determined by CFSE dilution. (B) BDC2.5 cell activation markers including CD44 and CTLA4 and (C) cytokine response including IFNγ (Axillary LN; Interaction= ns, NP vs peptide p=*0.027, HIP concentration= ns) and IL10. Statistical analysis was done using two-way ANOVA with Bonferroni post-test comparing peptide-NP and peptide at individual concentrations (* p<0.5 **p<0.01, ***p<0.001). Mean±SEM are shown; data are representative of 3 experiments (n=3 per treatment).